Cell Reports
Article

Cell PRESS
Open ACCESS

BIM-Mediated Membrane Insertion of the BAK Pore Domain Is an Essential Requirement for Apoptosis

Kathrin Weber,[1,3,4] Nicholas Harper,[1,3] John Schwabe,[2] and Gerald M. Cohen[1,2,*]
[1]MRC Toxicology Unit, University of Leicester, Hodgkin Building, Leicester LE1 9HN, UK
[2]Department of Biochemistry, University of Leicester, Henry Wellcome Building, Leicester LE1 9HN, UK
[3]These authors contributed equally to this work
[4]Present address: Molecular Signaling and Cell Death Unit, Department for Molecular Biomedical Research, VIB, Ghent University, Ghent (Zwijnaarde) 9000, Belgium
*Correspondence: gmc2@le.ac.uk
http://dx.doi.org/10.1016/j.celrep.2013.09.010

SUMMARY

BAK activation represents a key step during apoptosis, but how it converts into a mitochondria-permeabilizing pore remains unclear. By further delineating the structural rearrangements involved, we reveal that BAK activation progresses through a series of independent steps: BH3-domain exposure, N-terminal change, oligomerization, and membrane insertion. Employing a "BCL-X_L-addiction" model, we show that neutralization of BCL-X_L by the BH3 mimetic ABT-737 resulted in death only when cells were reconstituted with BCL-X_L:BAK, but not BCL-2/ BCL-X_L:BIM complexes. Although this resembles the indirect model, release of BAK from BCL-X_L did not result in spontaneous adoption of the pore conformation. Commitment to apoptosis required association of the direct activator BIM with oligomeric BAK promoting its conversion to a membrane-inserted pore. The sequential nature of this cascade provides multiple opportunities for other BCL-2 proteins to interfere with or promote BAK activation and unites aspects of the indirect and direct activation models.

INTRODUCTION

The dynamic interplay between pro- and antiapoptotic members of the BCL-2 family dictates life and death decisions. Activation of the proapoptotic BCL-2 proteins, BAK and BAX (the effectors), represents the pivotal step toward apoptosis by mediating mitochondrial outer membrane permeabilization (MOMP) (Chipuk and Green, 2008; Youle and Strasser, 2008). Despite their essential role in apoptosis, how effectors are activated by other BCL-2 family members remains controversial (Leber et al., 2007). According to the indirect model, antiapoptotic BCL-2 proteins sequester effectors to block their proapoptotic function. BH3-only proteins can displace BAK or BAX from their antiapoptotic counterparts, thereby facilitating their oligomerization and subsequent MOMP (Willis et al., 2005). A competing direct activation model proposes that effector function is triggered by activator BH3-only proteins, such as BIM and tBID (Kim et al., 2009; Ruffolo and Shore, 2003; Wei et al., 2000).

Although the underlying mechanism of activation remains unclear, effectors undergo major structural reorganizations in order to convert the monomeric, globular, closely packed protein into a highly ordered, multimeric mitochondrial permeabilizing pore. The association of BAK with antiapoptotic BCL-2 family members, as predicted by the indirect model, occurs through the canonical BH3:groove interface (Sattler et al., 1997; Willis et al., 2005). Because the BH3 domain is occluded in inactive BAK, exposure of the BH3 domain, which coincidentally results in the opening of the hydrophobic binding groove (BH1–BH3 domains), has to precede BCL-X_L association (Moldoveanu et al., 2006). This conformational change may be induced by direct association with activators either through the canonical BH3:groove interface or the BH3 trigger site (a hydrophobic cleft opposite the canonical groove formed by α1 and α6 helices; Czabotar et al., 2013; Leshchiner et al., 2013; Moldoveanu et al., 2013). The resulting conformation can then engage the BH3 domain of a neighboring effector protein to form a reciprocal, symmetric, BH3:groove dimer (Dewson et al., 2008). The assembly into high-molecular-weight complexes occurs through a second α6:α6 interface (Dewson et al., 2009). In addition, based on a structural similarity to α-pore-forming toxins (α-PFTs), execution of effector function may require membrane insertion of the central α5/α6 hairpin (pore domain) to form the mitochondria-permeabilizing pore (Annis et al., 2005; Griffiths et al., 1999; Makin et al., 2001; Muchmore et al., 1996).

To further delineate and characterize the steps required for the transition of native BAK into a membrane-permeabilizing pore, we combined biochemical and structural approaches to reveal a progressive sequence of (1) exposure of the BH3 domain, (2) N-terminal change, (3) oligomerization, and (4) insertion of the pore domain. By establishing a "BCL-X_L addiction" model system (Certo et al., 2006), we found that BCL-X_L sequesters preactive, BH3-domain-exposed BAK. Release of this checkpoint by

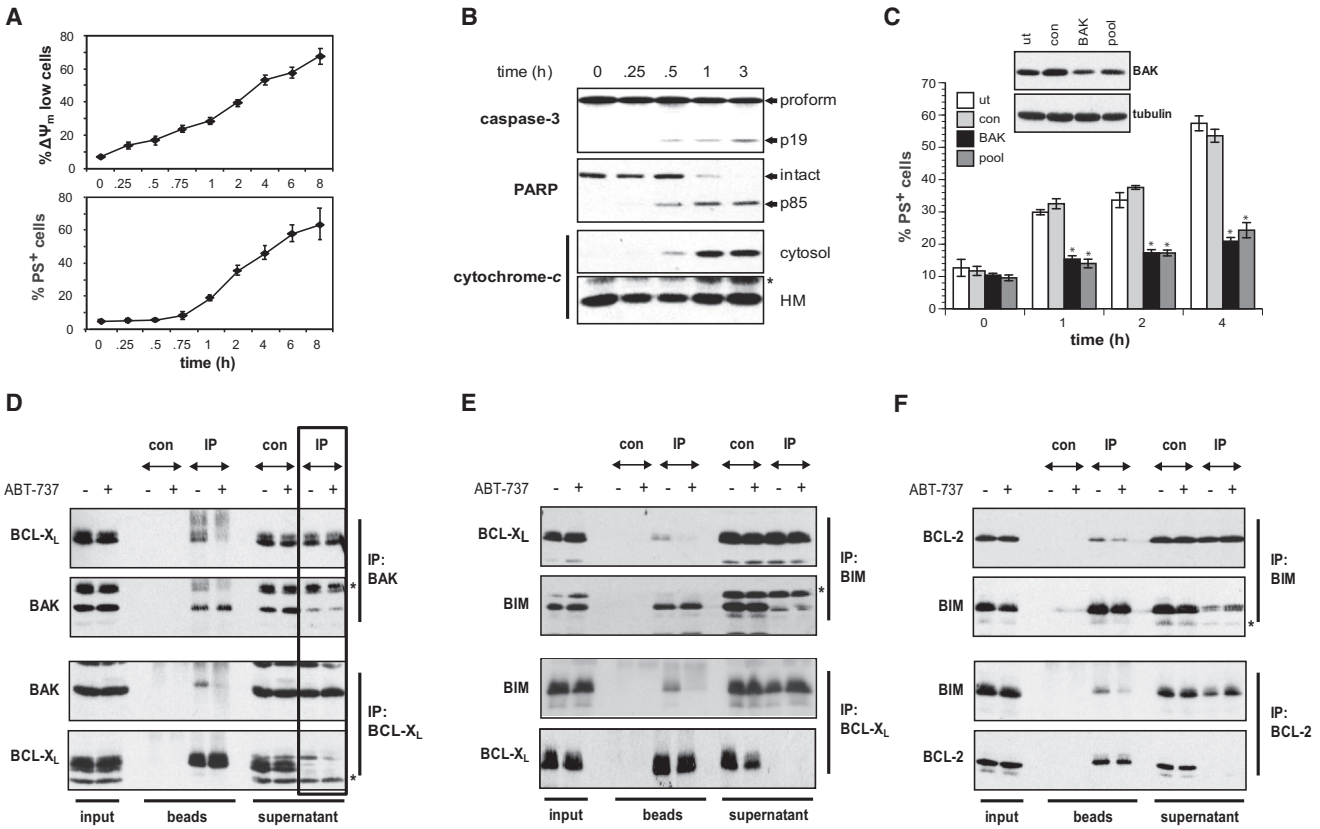

Figure 1. BAK and BIM Are Displaced from BCL-X_L by ABT-737

(A and B) ABT-737 triggers the intrinsic apoptosis pathway. (A) Jurkat cells were treated with ABT-737 (5 μM) and the percentage of apoptotic cells determined at the indicated times by using tetramethylrhodamine ethyl ester to measure mitochondrial membrane potential ($\Delta\Psi_m$) and Annexin V staining for the externalization of phosphatidylserine (PS). Data represent the mean ± SEM from eight different experiments. (B) Processing of caspase-3 and cleavage of PARP were analyzed following ABT-737 treatment. Cytochrome *c* release was assessed by digitonin fractionation. HM, heavy membrane fraction.

(C) ABT-737-induced cell death is BAK-dependent. Jurkat cells were transiently transfected with a single BAK siRNA (BAK), a pool of BAK siRNAs (pool), a control siRNA (con), or left untransfected (ut). After 48 hr, cells were treated with ABT-737 (5 μM) and PS externalization assessed at indicated times. *$p < 0.05$ compared to untreated cells. Levels of BAK were analyzed by western blotting.

(D) ABT-737 displaces BAK from BCL-X_L. Jurkat cells were treated with ABT-737 (5 μM), lysed in 1% CHAPS, and subjected to immunoprecipitation using either BAK or BCL-X_L antibodies. IP, immunoprecipitation. The asterisk denotes a nonspecific band.

(E and F) ABT-737 displaces BIM from BCL-X_L and BCL-2. Cells treated with ABT-737 (5 μM) were subjected to immunoprecipitation for either (E) BIM and BCL-X_L or (F) BIM and BCL-2. The asterisk denotes nonspecific bands.

See also Figure S1.

ABT-737 facilitates direct association with BIM promoting membrane insertion and subsequent cell death.

RESULTS

BAK Is Sequestered by BCL-X_L and Can Be Released by the BH3 Mimetic ABT-737

Although the activation of BAK may occur either directly or indirectly, a key feature of both models is the neutralization of antiapoptotic BCL-2 proteins by BH3-only proteins. To mimic this, we used ABT-737, which binds with high affinity to the hydrophobic groove of BCL-X_L, BCL-2, and BCL-w and induces apoptosis in a BAK and/or BAX-dependent manner (Oltersdorf et al., 2005; van Delft et al., 2006; Vogler et al., 2009). Jurkat cells exposed to ABT-737 exhibited classical apoptotic characteristics, including reduction in $\Delta\Psi_m$, increased phosphatidylserine (PS) externalization, cytochrome *c* release, and processing of caspase-3 and poly (ADP-ribose) polymerase (PARP) (Figures 1A and 1B). As these cells lack BAX, ABT-737-induced apoptosis would be predicted to be solely dependent on BAK (Shawgo et al., 2008). In agreement with this, suppression of BAK expression resulted in a marked decrease in PS externalization following ABT-737 treatment (Figure 1C).

According to the indirect activation model, BAK is held in check by antiapoptotic proteins (Ruffolo and Shore, 2003; Willis et al., 2005). Immunoprecipitations revealed that BAK was associated with BCL-X_L, but not BCL-2 or MCL-1 in Jurkat cells (Figure 1D; data not shown). ABT-737 antagonized BCL-X_L and efficiently displaced BAK compatible with features of the indirect model. Closer analysis of the supernatant fractions indicated that, although the target protein was completely depleted, a reciprocal reduction in its coprecipitated binding partner was

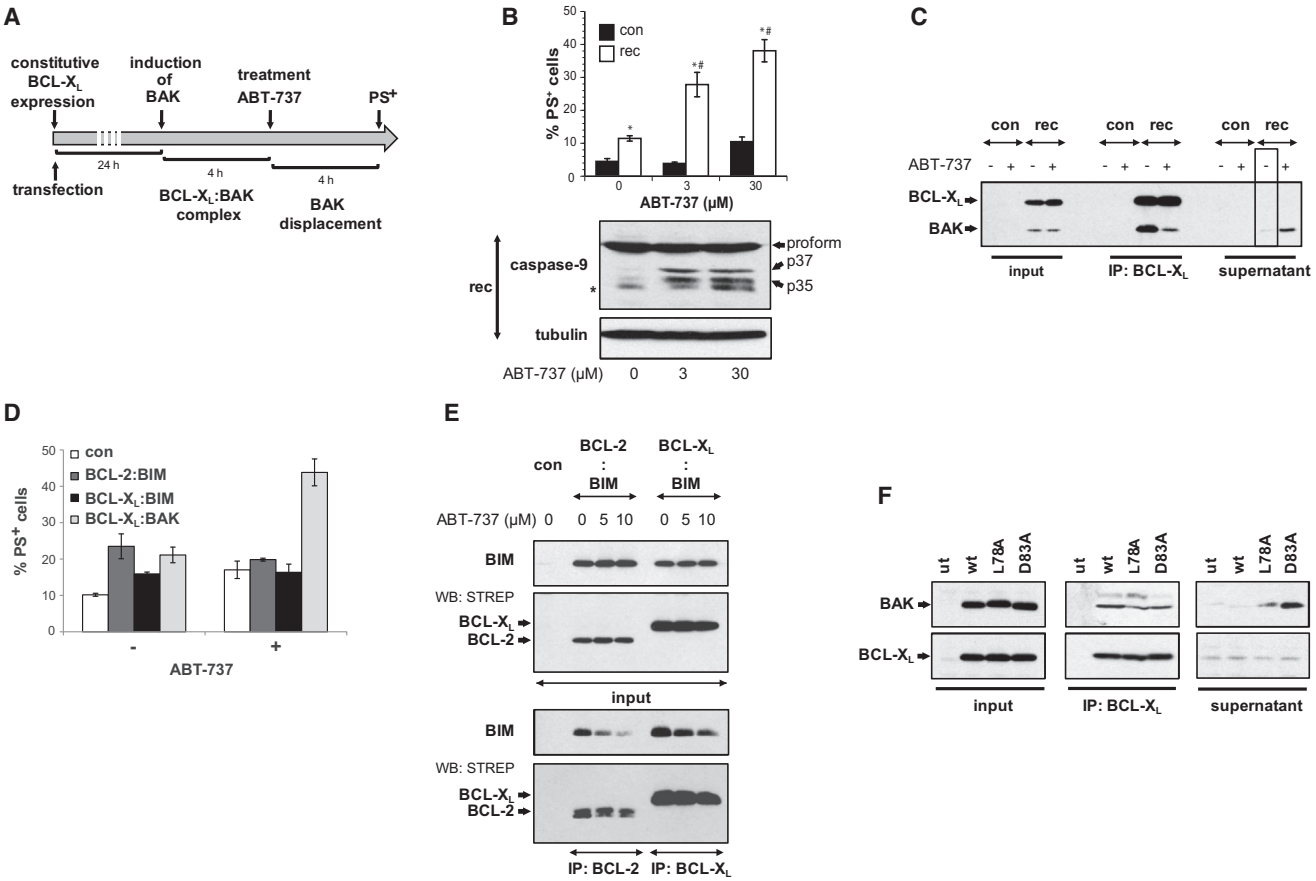

Figure 2. Reconstitution of BCL-X_L:BAK Complexes Sensitizes Cells to ABT-737

(A and B) Schematic representation of the BCL-X_L addiction model system as illustrated by the example of BCL-X_L:BAK. Bax and Bak DKO MEFs were transiently transfected with BCL-X_L (constitutive expression), BAK (under the control of tetracycline [TET]-inducible promoter) and a plasmid encoding the TET-repressor protein (TETR) to reconstitute BCL-X_L:BAK complexes (rec) or with empty vector (con). After 24 hr of BCL-X_L expression, BAK was induced for 4 hr with tetracycline and became complexed with by BCL-X_L. ABT-737 neutralizes BCL-X_L resulting in the displacement of BAK. (B) Reconstitution of BCL-X_L:BAK complexes sensitizes cells to ABT-737. DKO MEFs reconstituted with BCL-X_L:BAK complexes or MOCK-transfected (con) were treated with ABT-737 (3 and 30 μM) for 4 hr and cell death assessed by PS externalization (data points represent the mean ± SEM from three different experiments) and caspase-9 processing (asterisks denote nonspecific bands). *$p < 0.05$ compared to control; #$p < 0.001$ compared to untreated reconstituted cells.

(C) Induced BAK associates with BCL-X_L and is displaced by ABT-737. BCL-X_L:BAK-reconstituted or MOCK-transfected (con) DKO MEFs were treated with ABT-737 (3 μM) for 4 hr, lysed in 1% CHAPS, and subjected to immunoprecipitation using a BCL-X_L antibody.

(D and E) ABT-737-released BIM does not induce apoptosis in reconstituted cells. BAK was replaced with BIM, and HEK293T cells were reconstituted with BCL-X_L:BIM, BCL-2:BIM, or as a control BCL-X_L:BAK complexes. BIM-reconstituted cells were exposed to ABT-737 (5 or 10 μM) for 3 hr and (D) externalization of PS was determined (data points represent the mean ± SEM from three different experiments) or (E) BCL-2 or BCL-X_L was precipitated from CHAPS lysates using StrepTactin Sepharose.

(F) The BAK BH3 domain is involved in association with BCL-X_L. BAK BH3 mutants L78A and D83A were introduced into the reconstitution system in HEK293T cells or MOCK-transfected (con). Cells were lysed in 1% CHAPS and lysates subjected to immunoprecipitation using a BCL-X_L antibody.

See also Figure S2.

not observed (Figure 1D, box). Thus, only a discrete portion of BAK appeared to be complexed with BCL-X_L.

The direct activator BIM was also released from BCL-2 and BCL-X_L by ABT-737, and although its displacement was less efficient compared to BAK, released BIM could potentially act to "directly" activate inactive BAK (Figures 1E, 1F, and S1).

Reconstitution of BCL-X_L:BAK Complexes Results in Sensitivity to ABT-737

If the release of BAK from BCL-X_L is functionally important for ABT-737-induced apoptosis, then introduction of BCL-X_L:BAK complexes into resistant cells should sensitize them to ABT-737. To exclude interference from endogenous Bak or Bax, BCL-X_L:BAK complexes were introduced into Bax and Bak double-knockout (DKO) mouse embryonic fibroblasts (MEFs). As coexpressing BAK with BCL-X_L resulted in cell death, we first expressed BCL-X_L followed by tetracycline-induced expression of BAK (Figure 2A). Upon induction, BAK autoactivates but is then inhibited by a "sink" of BCL-X_L resulting in cells with BAK precomplexed to BCL-X_L exclusively. Reconstitution of BCL-X_L:BAK complexes sensitized DKO MEFs to ABT-737 as assessed by PS externalization and processing of caspase-9

(Figure 2B). As in this model system, all induced BAK was sequestered, effectively "addicting" the cells to BCL-X_L (Figure 2C, box), and ABT-737-induced cell death was a result of BAK release from BCL-X_L. Reconstitution of cells with MCL-1:BAK did not confer sensitivity to ABT-737 validating our model system (Figures S2A and S2B).

Introduction of BCL-X_L:BIM or BCL-2:BIM complexes into human embryonic kidney 293T (HEK293T) cells did not alter sensitivity to ABT-737 (Figures 2D and 2E). Thus, BIM released from BCL-2 or BCL-X_L did not appear to exert a direct activator function on endogenous BAK or BAX, further suggesting that the reconstituted BCL-X_L:BAK complexes are the preferential target of ABT-737. The model was then extended to characterize BCL-X_L:BAK complexes. BAK associates with BCL-X_L through the canonical BH3:groove association (Sattler et al., 1997). In agreement, introduction of BAK BH3 mutants L78A or D83A into the reconstitution system revealed that, whereas both coimmunoprecipitated with BCL-X_L, they were, in contrast to wild-type (WT) BAK, also recovered from the supernatant (Figure 2F). This implied both mutants displayed a reduced affinity for BCL-X_L and confirmed the requirement of the BH3 domain for complex formation. As this domain is occluded in inactive BAK, BCL-X_L sequesters a preactivated, BH3-domain-exposed conformation.

BAK N-Terminal Change Occurs Downstream of and Independent from BH3 Domain Exposure

In addition to BH3 domain exposure, conformational changes within the N-terminal region are also characteristic of BAK activation and are commonly determined by exposure of the Ab-1 epitope and increased trypsin sensitivity (Griffiths et al., 1999; Wei et al., 2000). Limited trypsin proteolysis on mitochondria isolated from ABT-737-treated Jurkat cells revealed a BAK cleavage fragment (p19), which was only detectable with the GLY82 antibody (epitope in the BH3 domain). In contrast, antibodies directed against the N-terminal region (NT and Ab-1) revealed a reduction in full-length BAK without detection of the p19 fragment, linking trypsin sensitivity to N-terminal change (Figures 3A, 3B, and S3). Together with formation of the p19 fragment, Ab-1-associated fluorescence was also detectable and occurred in the entire cell population, but not when cells were treated with an inactive enantiomer of ABT-737 (Figure 3C). Thus, N-terminal change required the neutralization of antiapoptotic proteins by ABT-737 and, by inference, this must occur downstream of BAK displacement from BCL-X_L.

To further explore the relationship between displacement and N-terminal change, we established a double immunoprecipitation procedure: the first was directed against Ab-1-exposed BAK, followed by a second, on the resulting supernatant, against BCL-X_L (Figure 3D). When Jurkat cells were lysed in CHAPS (to retain BAK in its native conformation), Ab-1 failed to precipitate BAK and the BCL-X_L:BAK complex was recovered from the resulting supernatant (Figure 3E, box). Thus, BAK complexed with BCL-X_L had not yet exposed the Ab-1 epitope. ABT-737 treatment resulted in the recovery of BAK by Ab-1, but BCL-X_L failed to coprecipitate suggesting that BAK exposes this epitope downstream of its release from BCL-X_L (Figure 3E). This was confirmed by the second immunoprecipitation, which recovered BCL-X_L without associated BAK. Taken together, these data demonstrated that the BAK N-terminal change occurred downstream of its displacement from BCL-X_L.

As the BAK BH3 domain is required for association with BCL-X_L, this further inferred that eversion of the BH3 domain occurred independent of and upstream of the N-terminal change. In addition, when the N terminus of BAK was artificially altered by Triton X-100, the BCL-X_L:BAK complex was recovered in both immunoprecipitations (Figure 3E; Dewson et al., 2008). Thus, under these conditions, BCL-X_L-sequestered BAK existed as a heterogeneous population of BH3-domain-exposed/Ab-1-exposed as well as BH3-domain-exposed/Ab-1-occluded conformations. Identical mixed conformations were also obtained by double immunoprecipitation with reconstituted cells solubilized in CHAPS and ABT-737 treatment, which resulted in conversion to an exclusively N-terminal changed population (Figure 3F). Thus, the N terminus can be altered either artificially with detergents or by "overexpression" without affecting the BH3:groove association highlighting the independence of both events.

BAK Oligomerizes following N-Terminal Change, a Pivotal, but Not Sufficient, Step toward MOMP

The oligomerization of BAK into dimers and high-molecular-weight complexes is a prerequisite for MOMP and can be assessed using the redox catalyst copper(II)(1,10-phenanthroline)$_3$ (CuPhe) (Dewson et al., 2008; Falke et al., 1988). In untreated Jurkat cells, CuPhe induced the formation of an intramolecular disulfide bond between N-terminal C14 and α6-localized C166 resulting in a faster migrating band on SDS-PAGE (M_X) (Figure 4A, left panel). ABT-737 treatment shifted the M_X form into disulfide-linked dimers (D) and higher molecular weight complexes (D^X). Reduction of disulfide bonds resulted in the detection of solely monomeric BAK (Figure 4A, right panel).

Oligomerization involves two distinct interfaces, the BH3 domain/groove and the α6 helix (Dewson et al., 2008, 2009). As the α6 helix is occluded by α1 helix in inactive BAK, the N-terminal change has to precede oligomerization. To analyze the chronology of the N-terminal change and oligomerization, BAK was restrained in its M_X conformation prior to activation. After incubation at 42°C to activate BAK (Pagliari et al., 2005), oligomer formation as well as cytochrome *c* release was reduced compared to "unrestrained" BAK (Figures 4B and 4C). These results indicated that the N-terminal change must precede oligomerization possibly to enable exposure of the oligomerization interface, the α6 helix, to the protein surface.

Interference with the BH3:groove interface by utilizing a BAK L78A or an N-terminal-truncated BAK ΔN83, which lacks a major part of the BH3 domain, did not impair oligomer formation (Figures 4D and S4B). Despite undergoing oligomerization, L78A BAK failed to induce apoptosis as assessed by PS externalization and cytochrome *c* release (Figures 4E, 4F, and S4A). Oligomerization was not an artifact as L78A BAK also underwent N-terminal change, a prerequisite for oligomerization (Figure 4F). Therefore, the ability to oligomerize did not appear to determine the proapoptotic activity of BAK suggesting the requirement of additional steps to convert BAK into a membrane-permeabilizing pore.

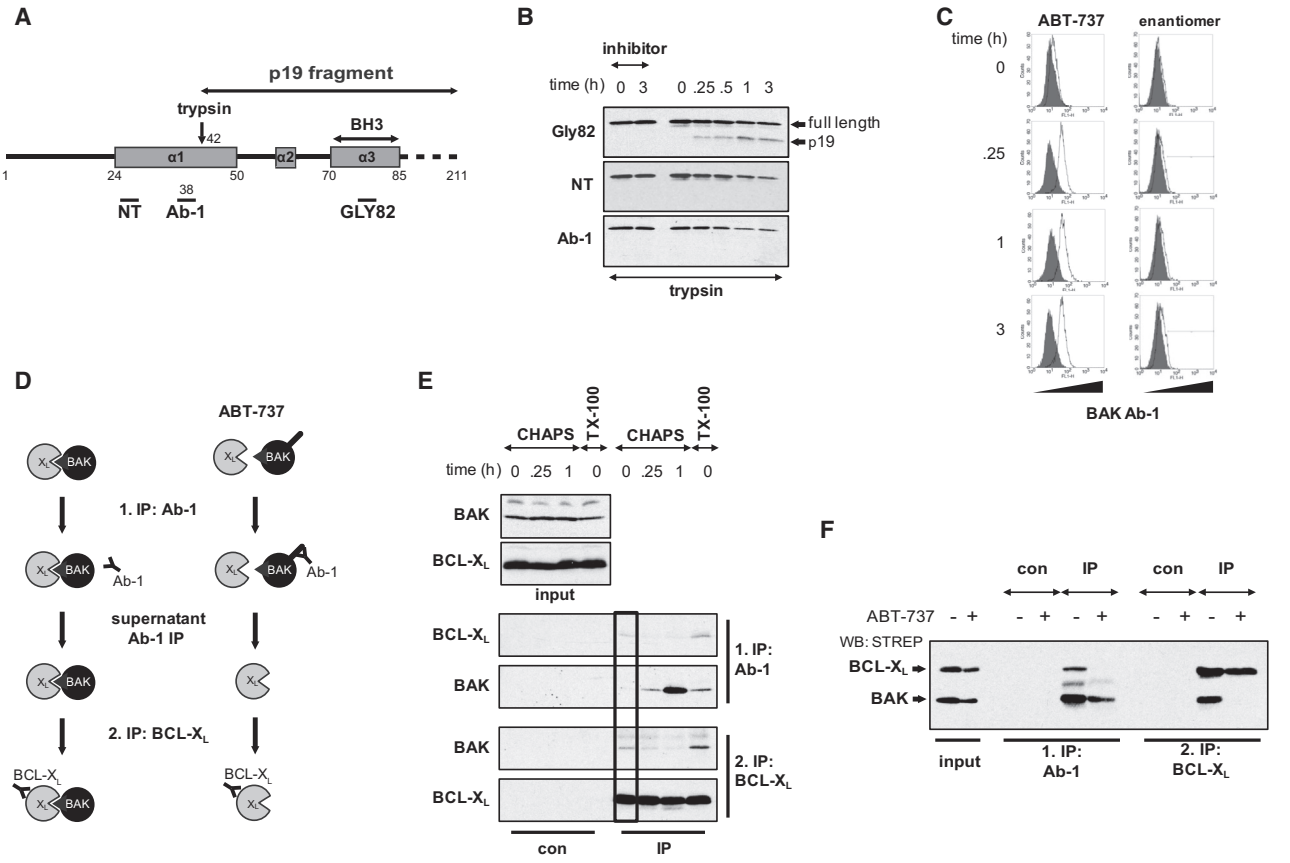

Figure 3. N-Terminal Change Occurs Downstream of the Release of BAK from BCL-X_L

(A) Schematic representation of BAK and location of Ab-1, NT, and GLY82 antibody epitopes are indicated. The trypsin cleavage site is marked by an arrow, and the resulting p19 fragment is shown.

(B) The BAK N terminus became trypsin-sensitive following ABT-737 treatment. Mitochondria from ABT-737-treated Jurkat cells (5 μM for indicated times) were isolated by Dounce homogenization and subjected to limited trypsin proteolysis. Cleavage of BAK was analyzed using a panel of BAK antibodies (Gly82, NT, and Ab-1). PefablocSC (inhibitor) was included as a control.

(C) The Ab-1 epitope is exposed following ABT-737 treatment. Jurkat cells were treated with ABT-737 (5 μM) or its inactive enantiomer (5 μM) for the indicated times. Cells were then labeled with BAK Ab-1/ALEXA488-labeled antibodies (open histogram) or secondary antibody alone (con, filled histogram) and analyzed for Ab-1-associated fluorescence by flow cytometry.

(D) Double immunoprecipitation procedure to determine N-terminal conformation of BCL-X_L-sequestered BAK. A first immunoprecipitation is directed against N-terminally changed BAK using the Ab-1 antibody. The resulting supernatant fraction is then subjected to a second immunoprecipitation against BCL-X_L.

(E) Ab-1 exposure occurs downstream of BAK displacement from BCL-X_L. ABT-737-treated Jurkat cells (5 μM for the indicated times) were lysed in 1% CHAPS or 1% Triton X-100 and lysates subjected to double immunoprecipitation.

(F) Reconstituted BAK is present as mixed population of N-terminal exposed and occluded forms. BCL-X_L:BAK-reconstituted or MOCK-transfected (con) DKO MEFs were treated with ABT-737 (30 μM) for 4 hr and lysed in 1% CHAPS. Lysates were subjected to double immunoprecipitation (as detailed in D).

See also Figure S3.

BAK Inserts Its Pore Domain into the Outer Mitochondrial Membrane

Membrane insertion of the BAX pore domain is associated with the formation of a MOMP-inducing pore (Annis et al., 2005; Antonsson et al., 1997; Schlesinger et al., 1997). We hypothesized that, following oligomerization, BAK inserts its pore domain into the membrane and the L78A mutant may be blocked at this stage accounting for its inactivity. The membrane topology of the α5/α6 hairpin in WT versus L78A BAK was analyzed by combining cysteine mutagenesis with 4-acetamido-4′-((iodoacetyl) amino) stilbene-2,2′-disulfonic acid (IASD) labeling (Annis et al., 2005; Krishnasastry et al., 1994). IASD only labels sulfydryl groups exposed to a hydrophilic environment resulting in the labeling of cysteine residues in the cytosol, the cytoplasmic boundary of a pore, or those facing the lumen of an aqueous pore. Cysteines embedded within the lipid bilayer or buried within a protein interface will be protected from IASD labeling (Figure 5A).

Cysteines were introduced in the pore domain of WT and L78A BAK using cysteine-deficient BAK (C14A/C166A) as a template. Insertions did not appreciably affect proapoptotic activity when overexpressed in DKO MEFs (Figure S5). As

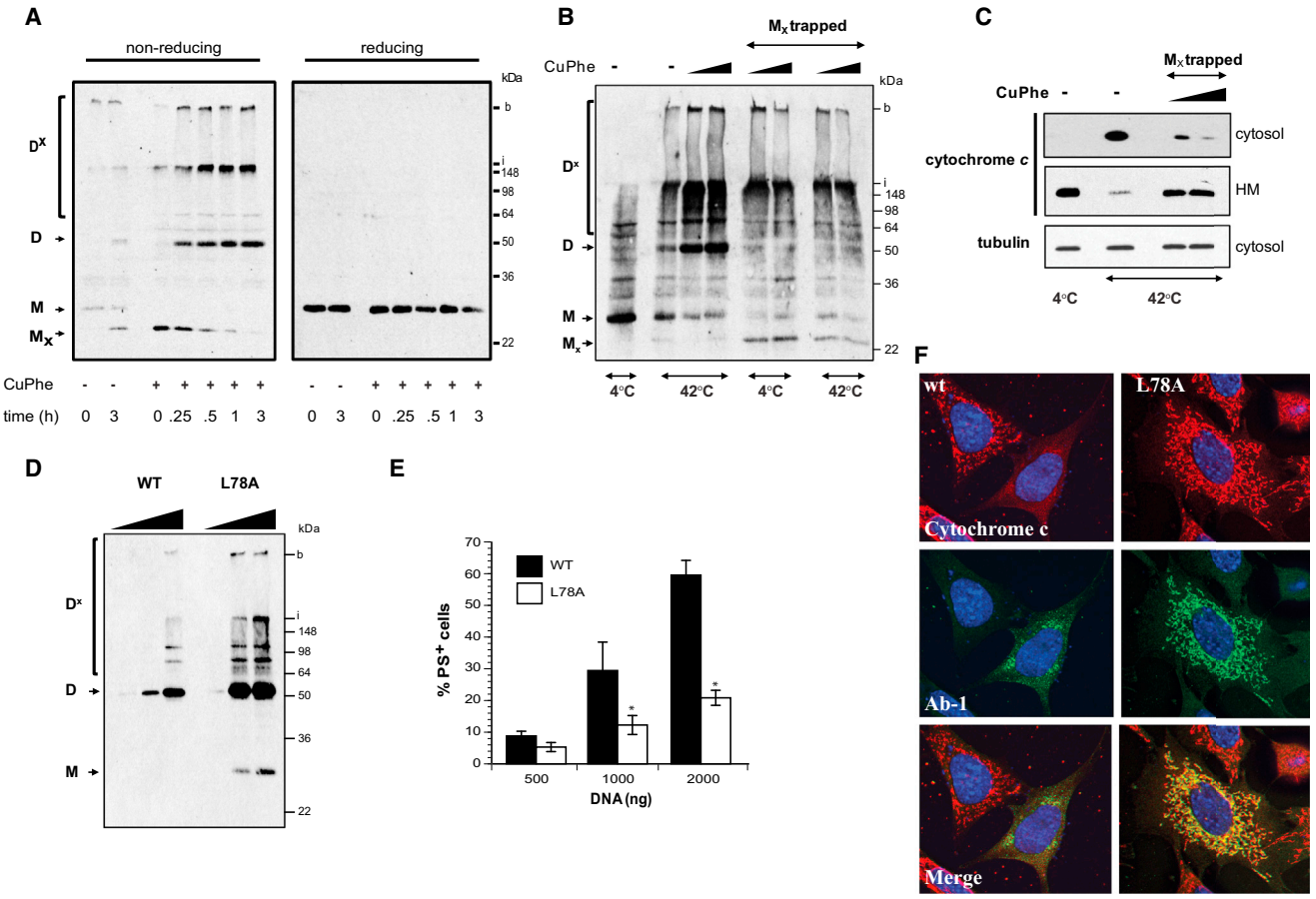

Figure 4. Oligomerization Does Not Represent the Final Step for Commitment to Apoptosis

(A) BAK oligomerizes during apoptosis. Jurkat cells were treated with ABT-737 (5 μM) for the indicated times. Mitochondria were then isolated and disulfide bonds introduced using CuPhe. Formation of BAK dimers and oligomers was analyzed by western blotting under nonreducing conditions (left panel) and specificity of bands confirmed using reducing conditions (right panel). M_x, intramolecular-disulfide bond, inactive BAK; M, monomeric BAK; D, intermolecular-disulfide bond, dimeric BAK; D^x, high-molecular-weight complexes; i, interface between stacking and running gel; b, bottom of the sample well.

(B and C) Restraining BAK in the M_X conformation impairs its proapoptotic function. Enriched mitochondrial fractions from control Jurkat cells were exposed to two different concentrations of CuPhe. "M_X-trapped" BAK was then heat-activated (42°C for 30 min) followed by analysis of (B) disulfide-linked oligomer formation and (C) cytochrome *c* release.

(D) BAK L78A still oligomerizes. WT and L78A BAK were transiently transfected into DKO MEFs. Oligomer formation was assessed 24 hr posttransfection using CuPhe and western blotting under nonreducing conditions.

(E) The BAK BH3 mutant, L78A, fails to induce apoptosis in Bax and Bak DKO MEFs. The asterisk denotes $p < 0.05$, and L78A was significantly different from wild-type.

(F) L78A BAK undergoes N-terminal change but fails to release cytochrome *c*. DKO MEFs were transfected with WT or L78A BAK for 24 hr; fixed, permeabilized, and stained with Ab-1 (green), Hoechst 33342, and anti-cytochrome *c* (red); and examined by confocal microscopy. L78A BAK-staining colocalized with mitochondria but did not release cytochrome *c* in contrast to WT BAK.

See also Figure S4.

BAK is constitutively membrane-anchored, a cysteine insertion at residue L195 within the transmembrane region (α9 helix) served as a control. Following overexpression in DKO MEFs, both WT and L78A L195C exhibited an unaltered mobility on SDS-PAGE compared to the unlabeled control (Figure 5B). This protection from IASD labeling represented membrane insertion, as solubilization in CHAPS resulted in an IASD-mediated increase in molecular weight. In contrast, the N-terminal endogenous cysteine C14 in both WT and L78A was labeled by IASD indicating the constitutive cytosolic localization (Figure 5B).

If the killing conformations of BAK and BAX are analogous, then the α5/α6 hairpin should be embedded in the membrane and, as a result, cysteines within these helices would be expected to be protected from IASD labeling (Annis et al., 2005). Conversely, if membrane insertion of the L78A mutant is impaired, then the corresponding cysteines would remain cytosolic and thus modified by IASD. In contrast a cysteine insertion at N124 (first N-terminal residue of the α5 helix) as well as the endogenous cysteine C166 (on the C-terminal end of the α6 helix) were modified by IASD in both WT and L78A BAK (Figure 5B). However, as both cysteines localize to the

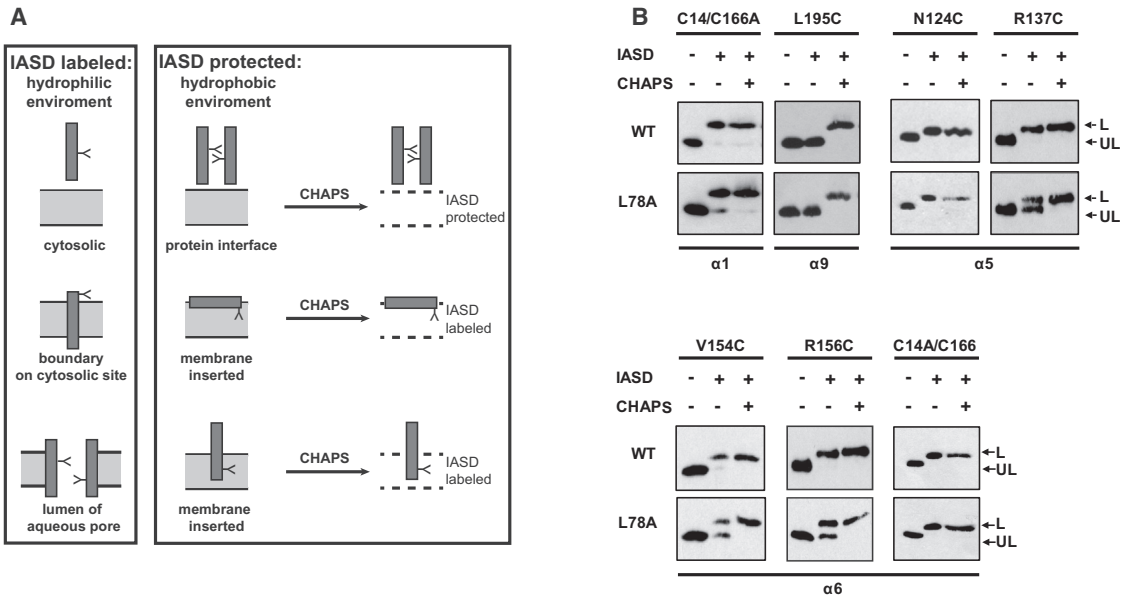

Figure 5. L78A BAK Adopts a Different Membrane Topology Compared to Wild-Type BAK

(A) Schematic representation of IASD accessibility/protection of cysteine residues in the context of a membrane environment. Cysteine residues, which are orientated to a hydrophilic environment, such as cytosol, lumen of an aqueous pore, or pore boundary, are accessible to IASD. In contrast, cysteines which are buried within hydrophobic protein interfaces or inserted into the hydrophobic membrane core are protected from IASD labeling. Both possibilities can be discriminated by solubilization in CHAPS.

(B) IASD-labeling pattern of L78A differs from WT BAK. Cysteines along the α5/α6 hairpin (pore domain) were introduced into cysteine-deficient WT or L78A BAK. Labeling controls were provided by L195C (within the α9 helix; transmembrane domain; constitutively membrane inserted) and the endogenous cysteine C14/C166A (N terminus; constitutively extramembranous). L78A and WT cysteine insertions were expressed in DKO MEFs at killing concentrations (1000 ng), HM fractions generated and labeled with IASD. Western blotting was used to detect labeled (L) and unlabeled (UL) species. A CHAPS-solubilized sample was included as a positive labeling control.

See also Figure S5.

extremities of the α5 and α6 helices in WT BAK, they could represent the cytoplasmic boundary of a membrane-inserted pore domain (Figure 5A).

Cysteine residues with a more centralized localization within the α5/α6 helices should therefore be protected in the "killing conformation" of WT BAK. Despite this, residues R137C (α5 helix) as well as WT V154C and R156C (both α6 helix) were also labeled by IASD (Figure 5B). However, the labeling pattern of the corresponding L78A mutants differed by the presence of an IASD-protected species. Solubilization with CHAPS resulted in a complete shift to a labeled band, thus excluding the occlusion of these cysteines in a protein-protein interface and demonstrating there was sufficient IASD for labeling. These results indicated that the pore domain of L78A adopts a different membrane topology to WT BAK possibly explaining opposing apoptotic activities of WT and L78A BAK.

BIM Promotes Insertion of the BAK Pore Domain

The different membrane topologies of WT compared to L78A BAK imply that adoption of the killing conformation was dependent on the BH3 domain. As the BH3 domain is part of the groove, the nonkilling, IASD-protected conformation of L78A could result from impaired engagement of a "ligand" BH3 domain which can be provided by a direct activator. In support of this hypothesis, we found that coexpression of the direct activator BIM with WT, but not L78A BAK, promoted cell death (Figure 6A). This synergism correlated with the coimmunoprecipitation of BIM with WT BAK, but not with the L78A mutant (Figure 6B). In this coexpression approach, WT BAK is already oligomerized when transfected alone indicating a role of BIM downstream of oligomerization possibly by promoting membrane insertion (Figure 6C).

In agreement, BIM altered the membrane topology of WT R137C or V154C by inducing a shift from the unlabeled to the IASD-labeled species (Figure 6D, box). Importantly, BIM did not alter the labeling pattern of the corresponding L78A mutants. However, both L78A and WT BAK gave a double band which was associated with cell death only with WT, but not L78A BAK. A similar pattern was also observed when WT BAK was overexpressed at an intermediate killing concentration (Figure S6A). Thus, the double band obtained with WT and L78A BAK may represent different membrane topologies.

To further investigate the effects of BIM on BAK, BIM expression was knocked down in the reconstitution system. Reduction of BIM expression resulted in a decrease of ABT-737-induced cell death (Figure 6E). We hypothesized that this effect should correlate with retention of WT R137C and V154C BAK in an IASD-protected nonkilling conformation (Figures 6D and S6A).

Agreeing with this, WT R137C was predominantly IASD-labeled and suppression of BIM resulted in reversion of

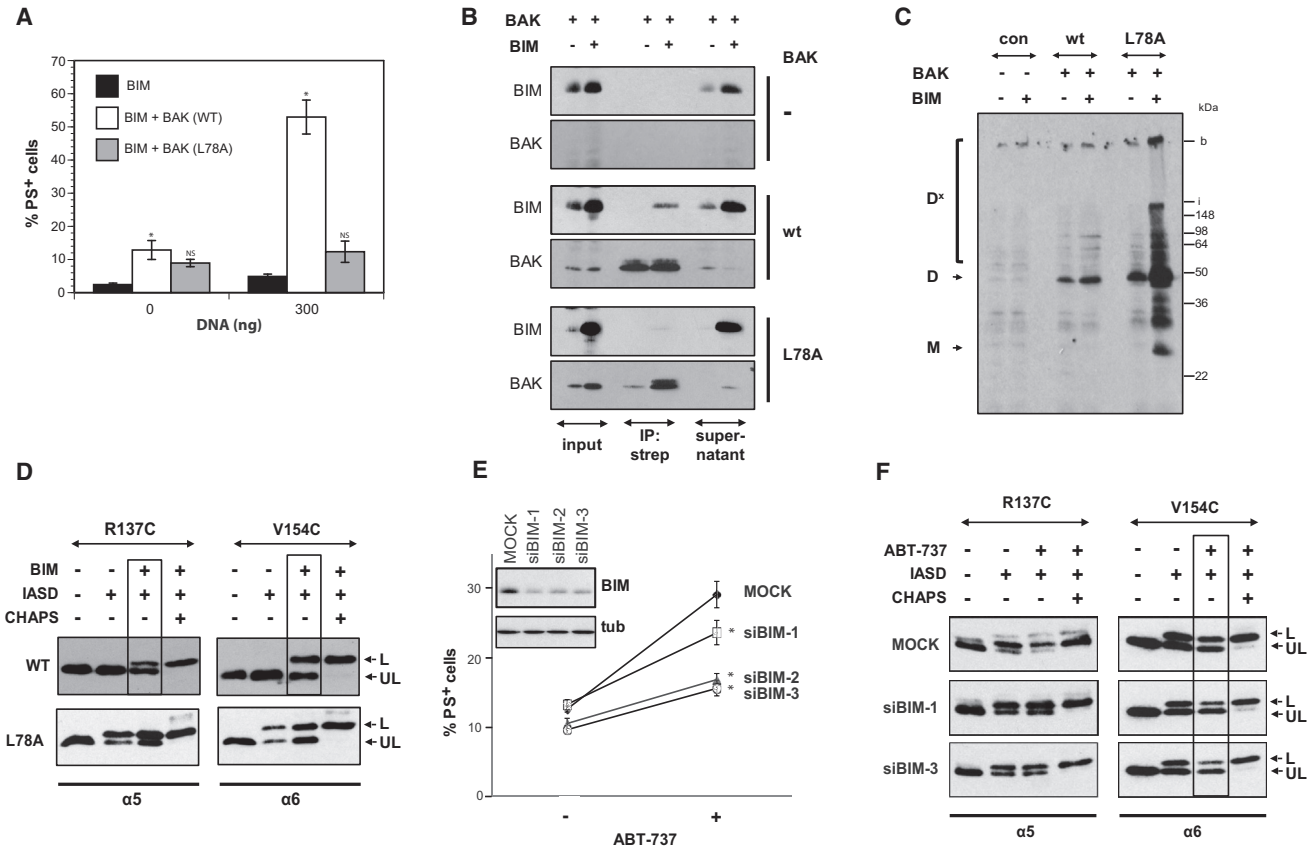

Figure 6. BIM Alters Membrane Topology of the α5/α6 Hairpin of WT but Not L78A BAK

(A) Coexpression of WT, but not L78A BAK, with BIM promotes proapoptotic activity. WT or L78A BAK was coexpressed with BIM in Bax and Bak DKO MEFs, and cell death was analyzed after 16 hr by PS externalization. The asterisk denotes $p < 0.05$ compared to Bim alone. NS, not significantly different compared to BIM alone.

(B) BIM coprecipitates with WT but not L78A. WT or L78A BAK were cotransfected with BIM in DKO MEFs. Cells were lysed in 1% CHAPS and BAK-precipitated using StrepTactin Sepharose. Interaction with BIM was analyzed by western blotting.

(C) BIM does not affect oligomerization of BAK. WT or L78A BAK was coexpressed with BIM and oligomerization assessed with CuPhe.

(D) BIM converts WT BAK from an IASD-unlabeled (UL) protected to labeled (L) conformation. WT or L78A R137C and V154C BAK were coexpressed at a sublethal concentration (500 ng) with BIM in DKO MEFs and HM fractions labeled with IASD.

(E) BIM siRNA results in reduced ABT-737 sensitivity in the reconstitution system. HEK293T cells were transfected with three different BIM siRNAs or con siRNA (MOCK). After 24 hr, cells were reconstituted with BCL-X_L:BAK complexes and treated with ABT-737 (5 μM for 3 hr). Cell death was determined by PS externalization. *$p < 0.05$ compared to MOCK-transfected cells.

(F) BIM siRNA reverts WT BAK to an IASD-protected (UL) conformation. Following transfection with two different BIM siRNAs, BCL-X_L:BAK R137C or BAK V154C complexes were reconstituted and treated with ABT-737 (5 μM for 3 hr). HM fractions were generated and subjected to IASD labeling.

See also Figure S6.

the labeled to an unlabeled species which was independent of release from BCL-X_L by ABT-737 (Figure 6F). When reconstituted, BCL-X_L sequestered oligomeric BAK and thus this does not contradict the proposed order of oligomerization followed by membrane insertion (Figures S1, 4A, and S6B). WT V154C gave a mixture of labeled and unlabeled species, and suppression of BIM reduced the IASD-labeled species, although this effect was only evident following ABT-737 treatment (Figure 6F, box). Taken together, these data revealed that the proapoptotic activity of WT BAK correlated with the conversion of an IASD-protected to a labeled conformation, which was promoted by interaction with BIM.

DISCUSSION

BAK and BAX are essential effectors of MOMP, the point of no return in apoptotic cell death, and as a consequence, their activation must be highly regulated. In this study, we demonstrate that activation of BAK involves several sequential but independent conformational changes, which provide different regulatory checkpoints mediated by members of the BCL-2 family. The antiapoptotic arm of this family functions to sequester a BH3-domain-exposed conformation of BAK preventing its further activation. BH3 mimetics, such as ABT-737, can release this checkpoint facilitating N-terminal change and oligomerization. The ability to oligomerize, however, did not correlate with

cell death, and formation of a MOMP-inducing pore required association with the direct activator BIM.

The Initial Steps: BH3 Domain Exposure, N-Terminal Change, and Oligomerization

In agreement with the indirect activation model, we validated a role for BCL-X_L and MCL-1, but not BCL-2, in inhibiting BAK activation (Ruffolo and Shore, 2003; Wei et al., 2000; Willis et al., 2005; Figures 1, 2, and S2). BAK associates with BCL-X_L through the canonical BH3:groove interface, which is stabilized by hydrophobic and electrostatic interactions. Interference with either (L78A or D83A BAK BH3 mutants) reduced binding to BCL-X_L (Figures 1D, 2C, and 2F; Sattler et al., 1997). By competing for the groove of BCL-X_L, ABT-737 displaced BAK from BCL-X_L further establishing the importance of the BH3:groove association (Figures 1D and 2C; Oltersdorf et al., 2005). In inactive BAK, key stabilizing hydrophobic residues within the BH3 domain face the protein core and association with BCL-X_L requires rotation of the BH3 domain-containing α3 helix to evert these residues to the protein surface. This change involves the opening of the otherwise occluded hydrophobic groove (BH1–BH3 domains). Thus, BCL-X_L does not sequester inactive BAK but a preactivated, BH3-domain-exposed/open-groove conformation.

In contrast to BAK, in BAX the α9 helix (transmembrane anchor) occludes the groove/BH3 domain. Its disengagement is required to expose the BH3 domain/groove, which may be allosterically induced by association of activators with the BH3 trigger side to induce an N-terminal change (Cartron et al., 2004; Gavathiotis et al., 2008). Thus, for BAX, N-terminal change precedes exposure of the BH3 domain/groove which is accompanied by translocation to the mitochondria. As BAK constitutively localizes to the mitochondria and the α1/α6 binding site is not as pronounced, it has been proposed that BAK can bypass this activation step resulting in constitutive exposure of the N terminus (Kim et al., 2009). However, several lines of evidence suggest that the N terminus is initially occluded. Exposure of a cryptic antibody epitope (Ab-1), increased trypsin sensitivity, as well as the loss of the M_x form are associated with the N-terminal change and exclusively occurred following ABT-737 treatment (Griffiths et al., 1999; Wei et al., 2000; Figures 3B, 3C, and 4D). By mapping the Ab-1 epitope to Y38 to the middle of the α1 helix, we attribute the increased accessibility to this epitope to a major reorganization of the N-terminal region (α1 and α2 helices) rather than the simple exposure (Figure S3). However, despite the close proximity of the N-terminal region with the BH3 domain, the N-terminal change occurred independent and downstream of BH3 domain exposure as BCL-X_L-sequestered BAK existed exclusively in an N-terminal-occluded conformation (Figures 3E and 3F). Furthermore, the N-terminal change is a prerequisite for oligomerization, as the formation of oligomers could be blocked by inhibiting the N-terminal change (Figures 3C, 4A, and 4B). This supports the proposed model for oligomerization as the N terminus occludes the α6 helix which represents the interface for BH3:groove-linked dimers to associate into oligomers (Dewson et al., 2008, 2009). However, the apparent, indispensable role of the BH3 domain in oligomer formation is unclear as both BAKΔN83 as well as BAK L78A both form oligomers (Figures 4D and S4B). Although BAK is oligomeric in the reconstitution system, BH3 domains appear to be available both to facilitate a BH3:groove association with BCL-X_L and to allow interaction with BIM (Figures 6B and S6B). Despite this, the BH3 domain clearly contributes to BAK proapoptotic function, as both BAKΔN83 as well as L78A lost their killing ability (Figures 4E and S4A). Thus, in analogy to BAX, a BH3-domain-dependent step must occur downstream of oligomerization (Kushnareva et al., 2012).

The BAK BH3 Mutant, L78A, Is Blocked at a Prepore Conformation

Structural similarities between α-PFTs prompted the hypothesis that BAK and BAX insert into the membrane to mediate MOMP (Muchmore et al., 1996). The membrane-inserting domains of α-PFTs are composed of a hydrophobic, central, helical hairpin which, in the native conformation, is surrounded by amphipathic helices. During activation, a series of conformational changes opens up these outer layers to expose the central hairpin, which then spontaneously penetrates the membrane (Parker et al., 1990). By analogy, during BAK activation, the outer α1 helix repositions away from the protein core exposing the α6 helix, which together with the α5 helix resembles the central hairpin of the PFTs. However, the pore domain of BAK is comprised of largely amphipathic helices, which are not expected to spontaneously membrane insert. The occlusion of polar surfaces within tertiary contact sides may energetically favor membrane insertion (Walker et al., 1992, 1995). By analogy, BAK assembled into high-molecular-weight complexes prior to membrane insertion (membrane anchored conformation; Figure S7i) and consequently could be labeled by IASD (Figures 5B and 6D; labeled band with L78A R137C and V154C). This effectively concentrated these subunits on the membrane surface potentially facilitating the coordinated membrane insertion (Figure S7ii). Evidence for a membrane-inserted conformation was suggested by the protection of R137C and V154C from IASD when using sublethal concentrations of WT BAK (Figure 6D) or in L78A BAK (Figures 5B and 6D). However, this labeling pattern was not associated with killing and consequently could not represent the final pore but rather a prepore conformation (Figures S6 and S7ii). In contrast, when WT BAK R137C and V154C were expressed at killing concentrations, they were accessible to IASD (Figure 5B). Considering that in active BAK the α5 and α6 helices have to adopt a transmembrane/membrane-inserted conformation (Oh et al., 2010), accessibility to IASD could be explained by the localization of these residues to the lumen of an aqueous pore. In support of this, amphipathic helices, like the pore domain of BAK, were shown to orientate their polar patches toward the lumen of the pore to expose nonpolar surface to the hydrophobic core of the bilayer (González-Mañas et al., 1993; Lakey et al., 1992). BAX is also described to form an ion-conductive, aqueous pore implying that polar residues within the pore domain must orientate to the lumen of the pore (Antonsson et al., 1997; Schlesinger et al., 1997). Thus, several lines of evidence point toward a membrane-inserted pore domain lining the lumen of an aqueous MOMP pore. This provides a possible explanation for the observed shift from unlabeled to labeled conformations which correlated with cell death.

The pore domain seemed to reorientate within the membrane from a state where the pore domain was "partially" inserted into the membrane (IASD-protected) to the mature MOMP-inducing pore (IASD-labeled). As pore formation appeared to be a highly dynamic process (Figure S6A), a continuous flux from membrane-anchored to pore conformation could occur, possibly explaining the detection of double bands under certain conditions.

BIM Promotes the Conversion of Prepore BAK to the Pore Conformation

Multidomain BCL-2 family members, such as BAK, are capable of acting both as ligand or receptor. Inserting its BH3 domain into the hydrophobic binding groove of antiapoptotic BCL-2 proteins affords BAK ligand characteristics, whereas the structurally juxtaposed BH1–BH3 domains form a hydrophobic groove, which can act as a receptor for the BH3 domain of direct activator proteins (Czabotar et al., 2013; Kim et al., 2009; Leshchiner et al., 2013). Activator engagement promotes the exposure of the effector BH3 domain and opening of the groove, thereby creating the interfaces required for oligomerization.

In our model, we could not find any direct activator role of BIM on endogenous BAK or BAX following its release from BCL-X_L (Figure 2D). However, the importance of direct activators in the initial activation of both BAK and BAX has been demonstrated recently using "BH3-stabilized α helices of BCL-2 proteins" or BH3 peptides on recombinant full-length or truncated effectors (Czabotar et al., 2013; Leshchiner et al., 2013; Moldoveanu et al., 2013).

In agreement, BIM synergized with BAK proapoptotic function as coexpression of both proteins enhanced and vice versa and decrease of BIM levels reduced cell death (Figures 6A and 6E). This effect was only evident with WT, but not L78A BAK, implying the requirement of an intact receptor surface to accommodate the BH3 domain of the activators. The direct activator role of BIM is attributed to the induction of BAK oligomerization (Cheng et al., 2001; Kim et al., 2009). However, in both model systems used, coexpression or reconstitution, BAK was oligomerized prior to BIM association (Figures 6C and S6B). Although we cannot exclude a possible involvement of BIM in the initial activation of BAK, our results suggest BIM can also act downstream of oligomerization in an unappreciated role to convert the membrane topology of oligomerized, partially membrane-inserted prepore BAK to the killing pore conformation. This hypothesis is supported by our finding that coexpression of BIM shifted WT R137C and V154C from an IASD-protected to a labeled species, whereas knockdown of BIM reversed this (Figures 6D and 6F). The N-terminal part of the α5 helix (amino acids 124–136) comprises the BH1 domain and thus participates in groove formation. Complete membrane insertion of this helix would effectively destroy the hydrophobic groove causing a loss of receptor characteristic. This would suggest that in prepore BAK, protection from IASD-labeling may represent the partial insertion of the α5 helix to maintain the structure and function of the groove and thus facilitate engagement with the BIM BH3 domain (Figures 6D and 6F). BIM could then promote conformational changes within the groove leading to complete insertion of the pore domain.

In summary, our results reveal that BAK activation is a complex process that includes a series of independent steps (Figure 7). Although BAK adopts an oligomeric conformation after its release from BCL-X_L, this conformation does not induce MOMP. We have identified a requirement for the direct activator BIM to convert oligomerized prepore BAK into a membrane-permeabilizing pore. Therefore, BAK activation does not exclusively occur through the direct or indirect activation models but rather combines aspects of both. These additional steps provide further unappreciated checkpoints to control activation and prevent unwanted/accidental cell death and also open up possible opportunities for tumors to deregulate apoptosis.

EXPERIMENTAL PROCEDURES

Detailed description of cell culture, immunoprecipitation, limited proteolysis, Ab-1 staining, transfection methods, and cell death analysis are provided in the Extended Experimental Procedures.

Constructs

pcDNA3.1, pcDNA4TO, pcDNA6, and pcDNA6-TetR were obtained from Invitrogen. Human BAK was cloned into pcDNA4TO with an N-terminal Strep-Tag II. Strep-Flag double-tagged BCL-X_L and BIM_{EL} were cloned into pcDNA6. Constructs were transiently transfected into Bax and Bak DKO MEFs (obtained from Drs. A. Strasser and D. Huang, The Walter and Eliza Hall Institute of Medical Research) using JetPrime (Polyplus) or HEK293T cells using Jet PEI (Polyplus) according to manufacturer's protocol. Where indicated, site-directed mutagenesis was performed using Quikchange Multi (Agilent Technologies), and all constructs were sequence-verified prior to use.

Reconstitution of BCL-X_L:BAK Complexes

Cells were transiently transfected with BAK, TetR, and BCL-X_L constructs at ratios 1:10 (BAK:TetR) and 1:1 (BAK:BCL-X_L). BAK was induced with tetracycline (4 μg/ml; Calbiochem) at 24 hr posttransfection for 4 hr prior to treatment with ABT-737.

Analysis of BAK Oligomers Using CuPhe

Formation of BAK high-molecular-weight complexes was analyzed using the redox catalyst CuPhe. Mitochondria-enriched fractions from Jurkat cells or digitonin-generated heavy membrane fractions from MEFs were solubilized in X-link Buffer (100 mM sucrose, 20 mM HEPES-KOH [pH 7.4], 2.5 mM $MgCl_2$, and 50 mM KCl) and incubated with CuPhe (20 mM 1,10 phenanthroline with 300 mM $CuSO_4$) for 30 min on ice. The reaction was then quenched by incubation with 100 mM EDTA for 15 min and mitochondria-enriched fractions recovered. Oligomerization of BAK was analyzed by SDS-PAGE under nonreducing conditions.

Assessment of BAK Membrane Topology Using IASD Labeling

BAK cysteine insertion mutants were transiently transfected into DKO MEFs or HEK293T cells. Heavy membrane fractions were obtained by mild digitonin lysis and washed with 10 mM dithiothreitol (DTT) to ensure reduction of sulfydryl groups. Pellets were resuspended in X-link buffer and incubated with 10 μM IASD for 30 min at room temperature. Reactions were quenched by addition of 100 mM DTT and mitochondria-containing fractions recovered. Resulting pellets were solubilized in 2% CHAPS and IASD modification analyzed by SDS-PAGE followed by western blotting on large-format SDS-PAGE gels. As controls, samples were left unlabeled or lysed in 2% CHAPS prior to IASD labeling.

SUPPLEMENTAL INFORMATION

Supplemental Information includes Extended Experimental Procedures and seven figures and can be found with this article online at http://dx.doi.org/10.1016/j.celrep.2013.09.010.

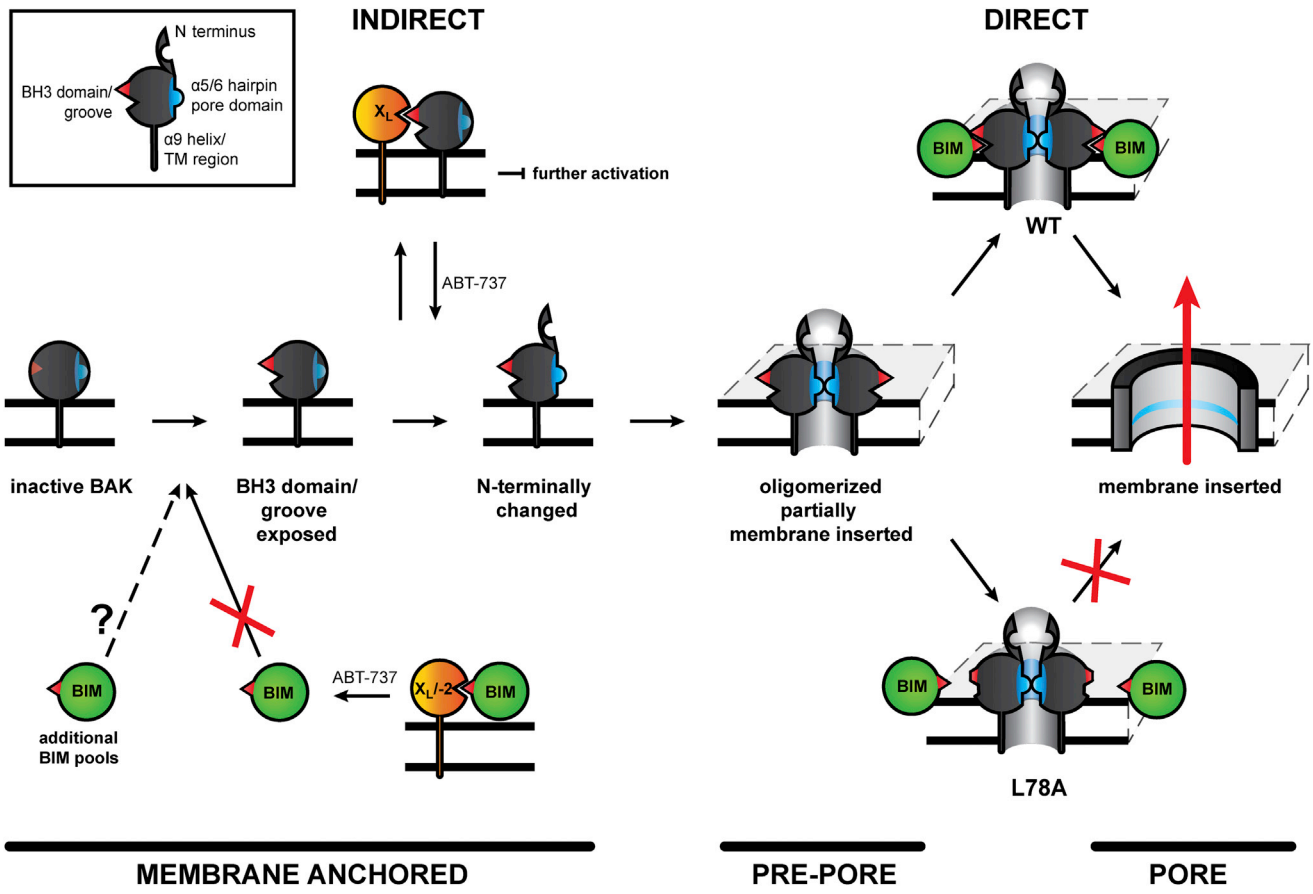

Figure 7. Schematic Model of BAK Activation

Inactive BAK is monomeric and adopts a closely packed, globular conformation with both the BH3 domain and groove occluded. Eversion of key hydrophobic residues within the BH3 domain to the protein surface results in groove opening and facilitates association with BCL-X_L through a BH3:groove interface. This interaction with BCL-X_L serves as a checkpoint to block further activation of BAK, thereby maintaining cell survival. Neutralization of BCL-X_L by ABT-737 results in the release of BAK, which then undergoes an N-terminal change followed by oligomerization. Activation of BAK up to this point is compatible with activation by the indirect model. Oligomerized BAK assumes a prepore conformation with the α5/α6 helices partially inserted in the mitochondrial membrane. Association with BIM results in the conversion of prepore WT BAK into a fully membrane-inserted, membrane-permeabilizing pore with the subsequent release of cytochrome *c* and the induction of apoptosis. BIM fails to interact with oligomerized and partially membrane-inserted BAK L78A, which remains in its inactive "prepore" conformation. Thus, the activation of BAK reflects an interplay between direct and indirect activation models.

See also Figure S7.

ACKNOWLEDGMENTS

We thank Dr. S. Rosenberg (Abbott Laboratories) for providing us with ABT-737, Dr. A. Strasser for the Bax and Bak DKO MEFs, Dr. S. Bratton (MD Anderson, Austin, Texas) for help with the statistical analysis, Prof. M. MacFarlane (MRC Toxicology Unit) for support of the work when under revision, and Dr. S. Varadarajan (MRC Toxicology Unit) for his help with immunofluorescent staining. This work was supported by the Medical Research Council and grants from the Marie Curie Research Training Network "ApopTrain" (to K.W. and G.M.C.).

Received: March 22, 2012
Revised: May 14, 2013
Accepted: September 6, 2013
Published: October 10, 2013

REFERENCES

Annis, M.G., Soucie, E.L., Dlugosz, P.J., Cruz-Aguado, J.A., Penn, L.Z., Leber, B., and Andrews, D.W. (2005). Bax forms multispanning monomers that oligomerize to permeabilize membranes during apoptosis. EMBO J. *24*, 2096–2103.

Antonsson, B., Conti, F., Ciavatta, A., Montessuit, S., Lewis, S., Martinou, I., Bernasconi, L., Bernard, A., Mermod, J.J., Mazzei, G., et al. (1997). Inhibition of Bax channel-forming activity by Bcl-2. Science *277*, 370–372.

Cartron, P.F., Gallenne, T., Bougras, G., Gautier, F., Manero, F., Vusio, P., Meflah, K., Vallette, F.M., and Juin, P. (2004). The first alpha helix of Bax plays a necessary role in its ligand-induced activation by the BH3-only proteins Bid and PUMA. Mol. Cell *16*, 807–818.

Certo, M., Del Gaizo Moore, V., Nishino, M., Wei, G., Korsmeyer, S., Armstrong, S.A., and Letai, A. (2006). Mitochondria primed by death signals determine cellular addiction to antiapoptotic BCL-2 family members. Cancer Cell *9*, 351–365.

Cheng, E.H., Wei, M.C., Weiler, S., Flavell, R.A., Mak, T.W., Lindsten, T., and Korsmeyer, S.J. (2001). BCL-2, BCL-X(L) sequester BH3 domain-only molecules preventing BAX- and BAK-mediated mitochondrial apoptosis. Mol. Cell *8*, 705–711.

Chipuk, J.E., and Green, D.R. (2008). How do BCL-2 proteins induce mitochondrial outer membrane permeabilization? Trends Cell Biol. *18*, 157–164.

Czabotar, P.E., Westphal, D., Dewson, G., Ma, S., Hockings, C., Fairlie, W.D., Lee, E.F., Yao, S., Robin, A.Y., Smith, B.J., et al. (2013). Bax crystal structures reveal how BH3 domains activate Bax and nucleate its oligomerization to induce apoptosis. Cell *152*, 519–531.

Dewson, G., Kratina, T., Sim, H.W., Puthalakath, H., Adams, J.M., Colman, P.M., and Kluck, R.M. (2008). To trigger apoptosis, Bak exposes its BH3 domain and homodimerizes via BH3:groove interactions. Mol. Cell *30*, 369–380.

Dewson, G., Kratina, T., Czabotar, P., Day, C.L., Adams, J.M., and Kluck, R.M. (2009). Bak activation for apoptosis involves oligomerization of dimers via their alpha6 helices. Mol. Cell *36*, 696–703.

Falke, J.J., Dernburg, A.F., Sternberg, D.A., Zalkin, N., Milligan, D.L., and Koshland, D.E., Jr. (1988). Structure of a bacterial sensory receptor. A site-directed sulfhydryl study. J. Biol. Chem. *263*, 14850–14858.

Gavathiotis, E., Suzuki, M., Davis, M.L., Pitter, K., Bird, G.H., Katz, S.G., Tu, H.C., Kim, H., Cheng, E.H., Tjandra, N., and Walensky, L.D. (2008). BAX activation is initiated at a novel interaction site. Nature *455*, 1076–1081.

González-Mañas, J.M., Lakey, J.H., and Pattus, F. (1993). Interaction of the colicin-A pore-forming domain with negatively charged phospholipids. Eur. J. Biochem. *211*, 625–633.

Griffiths, G.J., Dubrez, L., Morgan, C.P., Jones, N.A., Whitehouse, J., Corfe, B.M., Dive, C., and Hickman, J.A. (1999). Cell damage-induced conformational changes of the pro-apoptotic protein Bak in vivo precede the onset of apoptosis. J. Cell Biol. *144*, 903–914.

Kim, H., Tu, H.C., Ren, D., Takeuchi, O., Jeffers, J.R., Zambetti, G.P., Hsieh, J.J., and Cheng, E.H. (2009). Stepwise activation of BAX and BAK by tBID, BIM, and PUMA initiates mitochondrial apoptosis. Mol. Cell *36*, 487–499.

Krishnasastry, M., Walker, B., Braha, O., and Bayley, H. (1994). Surface labeling of key residues during assembly of the transmembrane pore formed by staphylococcal alpha-hemolysin. FEBS Lett. *356*, 66–71.

Kushnareva, Y., Andreyev, A.Y., Kuwana, T., and Newmeyer, D.D. (2012). Bax activation initiates the assembly of a multimeric catalyst that facilitates Bax pore formation in mitochondrial outer membranes. PLoS Biol. *10*, e1001394.

Lakey, J.H., González-Mañas, J.M., van der Goot, F.G., and Pattus, F. (1992). The membrane insertion of colicins. FEBS Lett. *307*, 26–29.

Leber, B., Lin, J., and Andrews, D.W. (2007). Embedded together: the life and death consequences of interaction of the Bcl-2 family with membranes. Apoptosis *12*, 897–911.

Leshchiner, E.S., Braun, C.R., Bird, G.H., and Walensky, L.D. (2013). Direct activation of full-length proapoptotic BAK. Proc. Natl. Acad. Sci. USA *110*, E986–E995.

Makin, G.W., Corfe, B.M., Griffiths, G.J., Thistlethwaite, A., Hickman, J.A., and Dive, C. (2001). Damage-induced Bax N-terminal change, translocation to mitochondria and formation of Bax dimers/complexes occur regardless of cell fate. EMBO J. *20*, 6306–6315.

Moldoveanu, T., Liu, Q., Tocilj, A., Watson, M., Shore, G., and Gehring, K. (2006). The X-ray structure of a BAK homodimer reveals an inhibitory zinc binding site. Mol. Cell *24*, 677–688.

Moldoveanu, T., Grace, C.R., Llambi, F., Nourse, A., Fitzgerald, P., Gehring, K., Kriwacki, R.W., and Green, D.R. (2013). BID-induced structural changes in BAK promote apoptosis. Nat. Struct. Mol. Biol. *20*, 589–597.

Muchmore, S.W., Sattler, M., Liang, H., Meadows, R.P., Harlan, J.E., Yoon, H.S., Nettesheim, D., Chang, B.S., Thompson, C.B., Wong, S.L., et al. (1996). X-ray and NMR structure of human Bcl-xL, an inhibitor of programmed cell death. Nature *381*, 335–341.

Oh, K.J., Singh, P., Lee, K., Foss, K., Lee, S., Park, M., Lee, S., Aluvila, S., Park, M., Singh, P., et al. (2010). Conformational changes in BAK, a pore-forming proapoptotic Bcl-2 family member, upon membrane insertion and direct evidence for the existence of BH3-BH3 contact interface in BAK homo-oligomers. J. Biol. Chem. *285*, 28924–28937.

Oltersdorf, T., Elmore, S.W., Shoemaker, A.R., Armstrong, R.C., Augeri, D.J., Belli, B.A., Bruncko, M., Deckwerth, T.L., Dinges, J., Hajduk, P.J., et al. (2005). An inhibitor of Bcl-2 family proteins induces regression of solid tumours. Nature *435*, 677–681.

Pagliari, L.J., Kuwana, T., Bonzon, C., Newmeyer, D.D., Tu, S., Beere, H.M., and Green, D.R. (2005). The multidomain proapoptotic molecules Bax and Bak are directly activated by heat. Proc. Natl. Acad. Sci. USA *102*, 17975–17980.

Parker, M.W., Tucker, A.D., Tsernoglou, D., and Pattus, F. (1990). Insights into membrane insertion based on studies of colicins. Trends Biochem. Sci. *15*, 126–129.

Ruffolo, S.C., and Shore, G.C. (2003). BCL-2 selectively interacts with the BID-induced open conformer of BAK, inhibiting BAK auto-oligomerization. J. Biol. Chem. *278*, 25039–25045.

Sattler, M., Liang, H., Nettesheim, D., Meadows, R.P., Harlan, J.E., Eberstadt, M., Yoon, H.S., Shuker, S.B., Chang, B.S., Minn, A.J., et al. (1997). Structure of Bcl-xL-Bak peptide complex: recognition between regulators of apoptosis. Science *275*, 983–986.

Schlesinger, P.H., Gross, A., Yin, X.M., Yamamoto, K., Saito, M., Waksman, G., and Korsmeyer, S.J. (1997). Comparison of the ion channel characteristics of proapoptotic BAX and antiapoptotic BCL-2. Proc. Natl. Acad. Sci. USA *94*, 11357–11362.

Shawgo, M.E., Shelton, S.N., and Robertson, J.D. (2008). Caspase-mediated Bak activation and cytochrome c release during intrinsic apoptotic cell death in Jurkat cells. J. Biol. Chem. *283*, 35532–35538.

van Delft, M.F., Wei, A.H., Mason, K.D., Vandenberg, C.J., Chen, L., Czabotar, P.E., Willis, S.N., Scott, C.L., Day, C.L., Cory, S., et al. (2006). The BH3 mimetic ABT-737 targets selective Bcl-2 proteins and efficiently induces apoptosis via Bak/Bax if Mcl-1 is neutralized. Cancer Cell *10*, 389–399.

Vogler, M., Weber, K., Dinsdale, D., Schmitz, I., Schulze-Osthoff, K., Dyer, M.J., and Cohen, G.M. (2009). Different forms of cell death induced by putative BCL2 inhibitors. Cell Death Differ. *16*, 1030–1039.

Walker, B., Krishnasastry, M., Zorn, L., and Bayley, H. (1992). Assembly of the oligomeric membrane pore formed by Staphylococcal alpha-hemolysin examined by truncation mutagenesis. J. Biol. Chem. *267*, 21782–21786.

Walker, B., Braha, O., Cheley, S., and Bayley, H. (1995). An intermediate in the assembly of a pore-forming protein trapped with a genetically-engineered switch. Chem. Biol. *2*, 99–105.

Wei, M.C., Lindsten, T., Mootha, V.K., Weiler, S., Gross, A., Ashiya, M., Thompson, C.B., and Korsmeyer, S.J. (2000). tBID, a membrane-targeted death ligand, oligomerizes BAK to release cytochrome c. Genes Dev. *14*, 2060–2071.

Willis, S.N., Chen, L., Dewson, G., Wei, A., Naik, E., Fletcher, J.I., Adams, J.M., and Huang, D.C. (2005). Proapoptotic Bak is sequestered by Mcl-1 and Bcl-xL, but not Bcl-2, until displaced by BH3-only proteins. Genes Dev. *19*, 1294–1305.

Youle, R.J., and Strasser, A. (2008). The BCL-2 protein family: opposing activities that mediate cell death. Nat. Rev. Mol. Cell Biol. *9*, 47–59.